Chemosphere 384 (2025) 144502

Contents lists available at ScienceDirect

Chemosphere

journal homepage: www.elsevier.com/locate/chemosphere

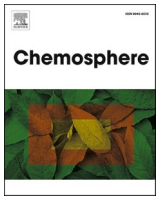

Bioaccumulations and biotransformations of azaspiracids from *Amphidoma languida* in the mussel *Mytilus edulis*

Elliot Murphy [a], Rafael Salas [b], Urban Tillmann [c], Jane Kilcoyne [b], Bernd Krock [c], Olivier P. Thomas [a,*]

[a] School of Biological and Chemical Sciences, Ryan Institute, University of Galway, University Road, H91 TK33, Galway, Ireland
[b] Marine Institute, Rinville, Oranmore, Co. Galway, H91 R673, Ireland
[c] Alfred Wegener Institut-Helmholtz Zentrum für Polarund Meeresforschung, Am Handelshafen 12, D-27570, Bremerhaven, Germany

HIGHLIGHTS

- Using a culture of Amphidoma languida known to produce azaspiracids 38 and 39, these metabolites were found to be bioaccumulated by mussels.
- AZA-38 and 39 were biotransformed by the mussel into oxidized and new derivatives of the recently described AZA-38 and 39.
- During a monitoring programme of mussels farmed in Ireland, AZA-38 and 39 were found in addition to the known AZA-1 and 2 raising concerns about shellfish toxicity.
- Their concentrations of AZA-38 and -39 in the shellfish were found to be significant lower than AZA-1 and 2.

GRAPHICAL ABSTRACT

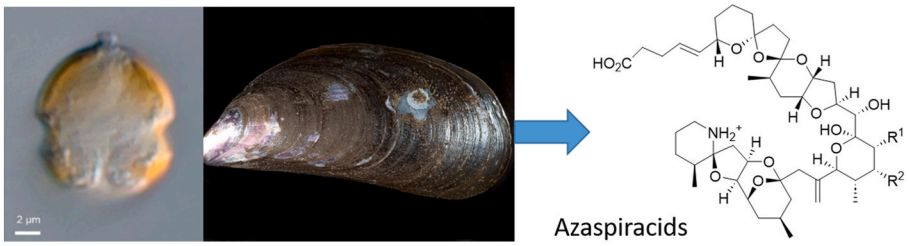

ARTICLE INFO

Handling editor: Derek Muir

Keywords:
Harmful algal blooms
Amphidoma
azaspiracid
Food safety
Marine toxins
Mytilus edulis
Bioaccumulation
Biotransformation

ABSTRACT

Azaspiracids are polyether marine algal toxins produced by several species of dinoflagellates from the family Amphidomataceae. Within the genus *Amphidoma*, *Am. languida* is the only species known so far to produce azaspiracids, while all the other toxin producers belong to the genus *Azadinium*. Strains of *Am. languida* collected in the Northeastern Atlantic have been found to produce AZA-38 and -39 as major metabolites. Cultures of *Am. languida* (24,000–30,000 cells mL^{-1}) fed to mussels (*Mytilus edulis*), confirmed the bioaccumulation of AZA-38 and -39 in shellfish tissues. AZA-38 and -39 were found to reach a combined 75.2 µg kg^{-1} (AZA-1 equivalents) in mussel tissue. The tentative identification of new derivatives resulting from the biotransformation of AZA-38 and -39 in the shellfish tissue was performed by LC-HRMS/MS. Although toxin concentrations in the tissue never reached AZA-1 regulatory limits, the study demonstrates that toxins from *Am. languida* can readily bioaccumulate and biotransform in shellfish and the toxicity of AZA-38 and -39 and their products of biotransformation should now be assessed. Importantly, a snapshot of biotoxin data from the Irish monitoring program in 2020 also identified AZA-38 and -39 in some shellfish species, albeit at low levels, from locations around the Southwest coast of Ireland.

This article is part of a special issue entitled: HABs & Biotoxins published in Chemosphere.

* Corresponding author.
E-mail address: olivier.thomas@universityofgalway.ie (O.P. Thomas).

https://doi.org/10.1016/j.chemosphere.2025.144502
Received 5 December 2024; Received in revised form 9 April 2025; Accepted 24 May 2025
Available online 5 June 2025

1. Introduction

Azaspiracids are a group of lipophilic toxins produced by dinoflagellates of the Amphidomataceae family. Their toxic effects were first observed when a diarrheic shellfish poisoning (DSP) event occurred in the Netherlands after consumption of Irish mussels but, in the absence of the known causative DSP toxins okadaic acid and dinophysistoxin-2, the conclusion was made that a new family of toxins must be present (McMahon et al., 1996). The causative agent of this toxicity, named azaspiracid (AZA), was isolated in 1998 from mussel tissue originating from Killary Harbour (Satake et al., 1998). The name aza-spiracid was derived from three chemical features of the molecule, namely spiro-ring assemblies and both a cyclic amine (indicated by the prefix "aza") and a carboxylic acid. The first proposed structure of AZA-1 was later revised through total synthesis (Nicolaou et al., 2004; Kenton et al., 2018). Subsequently, the structures of AZA-2 to −10, −26, −36, −37 and −59 were elucidated using NMR data and all other analogues were proposed using LC-MS/MS fragmentation data (Rehmann et al., 2008; James et al., 2003; Brombacher et al., 2002; Krock et al., 2015; Tebben et al., 2023). Following the first AZA poisoning event in 1995, similar events have occurred in other regions such as the Mediterranean Sea (France, Italy) and the Northwestern Atlantic Ocean (Furey et al., 2010). Shellfish contaminated with AZAs have been further detected in several coastal locations including Northwest Africa, Asia, South America and the West coast of Europe (Taleb et al., 2006; Alvarez et al., 2010; Economou et al., 2007; Álvarez-Muñoz et al., 2016; Kim et al.). *Azadinium spinosum*, discovered off the southeast coast of Scotland, was found to be the causative organism in the production of AZA-1 and -2 in 2009 (Tillmann et al., 2009; Krock et al., 2008). The number of reported AZA analogues has reached more than 60, largely as products of biotransformation in animal tissues but also from laboratory cultures (Rehmann et al., 2008; James et al., 2003; Ofuji et al., 1999, 2001; Lehane et al., 2004; Volmer et al., 2002; Krock et al., 2019; Kilcoyne et al., 2018; Sandvik et al., 2021). Other species of Amphidomataceae family have been found to produce close structural analogues of AZA-1. AZA-2, -11, −33, −34, −36, −37, -40–42, −48, −59 and −62 were identified from strains of *Azadinium poporum*, 3-*epi*-AZA-7 and AZA-54–58 were identified from strains of *Azadinium dexteroporum* from the Mediterranean Sea while strains of *Amphidoma languida* originating from Irish and Norwegian waters mainly produce AZA-38 and -39, and a strain isolated from the Spanish coast produces AZA-2 and -43 (Tillmann et al., 2017, 2018; Krock et al., 2012; Rossi et al., 2017).

In efforts to protect consumer health and maintain confidence in shellfish, legislation requiring the monitoring of shellfish samples has been implemented in Europe (Hoagland et al., 2006; Gerssen et al., 2010). Of the many identified AZAs, regulation currently explicitly requires the monitoring of only AZA-1–3. Concentrations of AZA equivalents (sum of AZA-1–3, corrected for their toxic equivalence factors) over 160 μg kg^{-1} of mussel meat are deemed too toxic for human consumption (Gerssen et al., 2010). Regulation (EC) No 2074/2005 states that the maximum levels of monitored toxins are provisional and should be amended to conform to new scientific findings (Visciano et al., 2016). Therefore, there is a need to identify new and emergent azaspiracid toxins and investigate their potential threat to human health and to the shellfish industry. With the emergence of novel toxic species and increased prevalence of bloom events, the pressure is now on research and development to identify which toxins should be included in routine monitoring programs.

Shellfish such as the blue mussel *M. edulis* were found to bioaccumulate and biotransform ingested AZA -1, −2 and −59 in multiple feeding studies with *Az. spinosum* and *Az. poporum* (Jauffrais et al., 2012; Salas et al., 2011; Krock et al., 2024). Once ingested, oxidation occurs in ring E with some hydroxylation observed at C-3 and C-23, and oxidation and decarboxylation at the methyl attached at C-22 of the structure of AZA-1 below (Fig. 1). Carboxylation was proposed as the more likely biotransformation of AZAs in blue mussels (Rehmann et al., 2008; Jauffrais et al., 2012; McCarron et al., 2009; Kittler et al., 2010; O'Driscoll et al., 2011). *In vitro* metabolism studies using mussel hepatopancreas proteins also identified intermediates of the carboxylated AZA-17 and -18, 22α-hydroxymethylazaspiracids AZA-65 and -66 (Sandvik et al., 2021). *Am. languida* is another species that could potentially bioaccumulate mussels in Ireland. This species has been reported to be widely distributed around the Irish coast and AZA intoxications through this species are therefore a matter of concern (Wietkamp et al., 2020). Field sampling has shown that shellfish contamination with AZAs from a Spanish strain of *Am. languida* has already been detected (Tillmann et al., 2017). Unlike AZA -1, −2 and −3, already proven to be toxic, AZAs from the Irish strain of *Am. languida* have yet to be tested for toxicity. The first bulk culture of *Am. languida* was recently reported and led to the revision of the structure of AZA-39 (Salas et al., 2023).

The aim of this study was to determine whether AZA-38 and -39 produced by *Am. languida* were bioaccumulated in mussel tissues. If retained we proposed to assess whether these toxins undergo the typical biotransformations observed for AZA-1 and -2 (Sandvik et al., 2021). We then assessed the effects of cooking through the analysis of the azaspiracid content after heating. Finally, a survey of historical shellfish samples was performed using LC-MS/MS analysis to assess whether AZA-38 and -39 and other derivatives were present in shellfish tissues provided to the Irish shellfish monitoring program led by the Marine Institute.

2. Materials and methods

2.1. Chemicals and reagents

All solvents (pestican-grade) were obtained from Labscan (Dublin, Ireland). Distilled water was purified further using a Barnstead nanopore diamond UV purification system (Thermo Scientific, Iowa, USA). Formic acid (>98 %) (Sigma-Aldrich, Missouri,USA), ammonium formate (>98 %) (Sigma-Aldrich, Missouri,USA). Certified reference material (CRM)s for AZA1 and -2 were obtained from the National Research Council (Halifax, NS, Canada).

2.2. Culture of Am. languida

The strain of *Amphidoma languida* (Z-LF-9C9) was isolated from the North Sea off the Danish coast at 56°07′N, 07°28′E and is fully described elsewhere (Tillmann et al., 2015). The strain was grown in K medium with no ammonia and an organic phosphate source (β-glycerol-phosphate) until appropriate concentrations and quantities of cells were reached. The culture was then bulked up using a modified K medium recipe (K-modified) which included tris base and Na_2SeO_3 enrichment (1.29 g L^{-1}) but no NH_4Cl. The culture was grown in a walk-in incubator with 16:8 h day/night cycle, and kept at 18.0 °C with an average photon flux density of 16.2 μmol (m^2 s^{-1}). The culture was maintained until cell concentrations reached 20,000 cells mL^{-1}. A growth tank of 180 L, containing 25 L of K-modified medium, was then inoculated with 20 L of culture at a concentration of 20,000 cell mL^{-1}. The pH was monitored throughout the culture growth and controlled using CO_2 diffusion. The culture was mixed through aeration. The volume of the PBR was slowly brought up to 180 L over 5 days, while maintaining a concentration of <40,000 cells mL^{-1} to limit collapse known to occur at higher concentration.

2.3. Experimental design

A total number of 36 individual mussels (*M. edulis*) were harvested off the West coast of Ireland. Mussels were inspected for any fouling organisms and placed in a 10 L plastic container filled with sterile seawater (salinity of 35) in the walk-in incubator at 18 °C. The experiment consisted of a 24 h feeding experiment with monocultures of *Am.*

languida to study feeding activity and toxin uptake and bioconversion.

Algal aliquots were collected from the photobioreactor and their cell densities were recorded using a Sedgewick–Rafter cell counting chamber (Pyser-SGI, Kent, UK) ranging from 24,000 to 30,000 cells mL^{-1}. A subset of the culture was then transferred to 5 L polyethylene jugs. Sterile seawater was added to the control. A volume of 10 mL of culture was collected in triplicate and stored at −20 °C from each replicate and control to test for initial concentration of AZAs. Mussels (n = 9) were submerged in 5 L polyethylene jugs to form 3 replicates and 1 control. Each replicate was mixed throughout the experiment using aeration via airstones, tygon tubing and air pumps. During the first 2 h of the experiment, 1 mL aliquots of seawater were collected from each flask every 20 min using a 1 mL pipette (Eppendorf, Cambridge, UK) and preserved with Lugol's iodine (Clintech, Dublin, Ireland) 1 % final concentration to estimate cell concentrations of *Am. languida* during the experiment. After 2 h, aliquots were collected every hour for a further 3 h and finally at 24 h.

After 24 h, 3 mussels were removed from each replicate and control. The mussels were measured and weighed before being dissected with the hepatopancreas and remainder tissue retained from each replicate. After removing the mussels, the culture (5 L) that they were submerged in was filtered to recover the particulate matters ('Bio-deposits' in Table 2) using GF/C Whatman (1.2 μm, 47 mm diameter) glass microfiber filters under vacuum. The filters were then extracted with 10 mL of MeOH and the AZA content was quantified. A final sample (10 mL) was collected in triplicate from the remaining filtrate to quantify the dissolved AZAs in the filtrate ('Filtrate T24' in Table 2), the AZAs were concentrated using the SPE method and analyzed via LCMS.

2.4. Am. languida cell counts

Cell counts of the 1 mL Lugol's preserved aliquots were carried out using a Sedgewick–Rafter cell counting chamber (Pyser-SGI, Kent, UK) for each flask at each time interval using an inverted optical microscope Leica DMI 6000B (Leica, Wetzlar, Germany).

2.5. Filtration rate

Filtration rate or clearance rate was calculated using the equation proposed by Frost et al. and has previously been used in a mussel feeding study by Krock et al.(Krock et al., 2024; Frost, 1972).

$$f = \frac{V(\ln C_0 - \ln C_t)}{n^* t}$$

Where C_0 and C_t = algal concentration at time 0 and time t, V = volume of water, and n = number of animals.

2.6. Solid phase extraction (SPE) protocol used for desalting prior to AZA quantitation

A volume of 10 mL of samples were collected from each of the three culture replicates and the control. The samples were stored at −20 °C until analyzed. Prior to analysis, they were defrosted and loaded onto a 1-g 6 mL Oasis Bond Elut cartridges (Mega BE SPE, Agilent Technologies, Mississauga, Ontario, Canada), previously conditioned with MeOH (6 mL) and H_2O (6 mL). The cartridge was then washed with H_2O (6 mL) followed by the elution of 15 mL of MeOH to recover the AZA content. The eluent was evaporated to dryness using miVac QUATTRO concentrator (Genevac, Ipswich, England). The samples were then resuspended in 10 mL of MeOH and sonicated for 10 min (Elma S 100 Elmasonic, Elma Schmidbauer GmbH, Singen, Germany). A volume of 1 mL was transferred to a 1.5 mL vials for LC-MS/MS analysis.

2.7. Dissection of mussels and toxin analysis of shellfish tissues

In this part, we used a similar method as the one reported in Salas et al. (2011). After 24 h, 3 of the 9 mussels in each replicate culture were collected from the jugs, weighed and measured (length, width and height), then dissected, separating the hepatopancreas from the remainder of the tissue before both were placed in 50 mL conical centrifuge tubes (Corning, New York, USA). For the extraction the samples were thawed at room temperature before a volume of 1.5 mL MeOH was added to each tube containing the hepatopancreas extracts and the sample was homogenized using an Ultra-Turrax (T25 Basic IKA1-Werke, Germany) at 11,000 rpm for 1 min. Samples were then centrifuged in a Heraeus Multifuge 3S–R (Heraeus, Hanau, Germany) at 4500 rpm for 5 min. The supernatant was decanted into 5 mL volumetric flasks (Hirsmann-Techcolor, Heilbronn, Germany) and this step was repeated twice for each pellet. For the remainder tissue, a volume of 3 mL MeOH was added to each tube and the sample was again homogenized using an Ultra-Turrax (T25 Basic IKA1-Werke, Germany) at 11,000 rpm for 1 min. Samples were again centrifuged in a Heraeus Multifuge 3S–R (Heraeus, Hanau, Germany) at 4500 rpm for 5 min. The

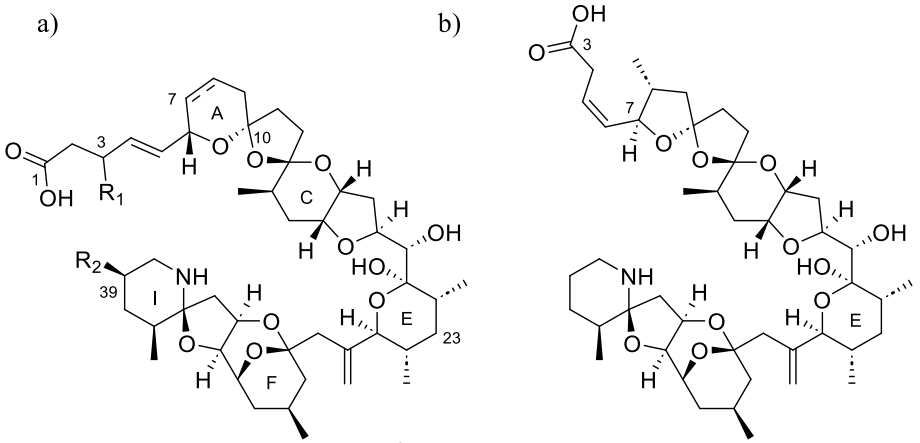

	$\Delta^{7,8}$	R_1	R_2
AZA-1	yes	H	CH_3
AZA-37	no	OH	H
AZA-38	no	H	H

Fig. 1. Structure of a) AZA-1, AZA-37 and AZA-38, b) revised structure of AZA-39 (Salas et al., 2023).

supernatant was decanted into 10 mL volumetric flasks (Hirsmann--Techcolor, Heilbronn, Germany) and this step was repeated twice for each pellet. The volume was then brought up to the mark using pestican grade MeOH, inverted 5 times for each and filtered through 0.22 mm filters (Sartorius, Surrey, UK) into HPLC vials (AGB, Dublin, Ireland) to be run on the LC–MS/MS.

2.8. Toxins determination by liquid chromatography with mass spectrometry detection (LC-MS/MS)

Quantification of toxins was performed on an Acquity UPLC coupled to a Xevo G2-S QtoF (Waters, Manchester, UK). All quantitation of AZAs were recorded in MS/MS mode with full scans from *m/z* 200–1200 +ESI mode. MS/MS spectra were collected in targeted MS/MS mode scanning for the target masses of potential AZA analogues with a window of ±0.5 Da (*m/z* 830.5, 816.5, 846.5, 860.5, 876.5, 832.5, 846.5, 802.5 and 818.5). The reference compound used for calibration was leucine encephalin. The cone voltage was 40 eV, collision energy was 50 eV, the cone and desolvation gas flows were set at 100 and 1000 L h^{-1}, respectively, with a source temperature of 120 °C. The quantitation was performed in MSe mode, using Targetlynx software. All toxins were quantitated against AZA-1 using full scan peak areas.

A binary gradient elution was used with mobile phase A consisting of H_2O and phase B of 95:5 CH_3CN/H_2O, both containing 2 mM ammonium formate and 50 mM formic acid. The quantification of AZAs was performed with UPLC column (50 mm × 2.1 mm i.d., 1.7 μm, Acquity UPLC BEH C_{18} Waters, Wexford, Ireland). Initial conditions of 30 % B were used, followed by a linear gradient to 90 % over 6 min at flow rate of 0.3 mL min^{-1}, held for 0.5 min, and returned to the initial conditions and held for 1 min to equilibrate the system. The injection volume was 2 μL and the column and sample temperatures were 25 °C and 6 °C, respectively. This method was used to quantify the AZA content in the culture (T0), Filtrate (T24), bio-deposits, mussel tissues, and farmed shellfish samples provided to the marine institute for monitoring.

2.9. HRMS/MS data obtained to characterize the AZA

Liquid chromatography with high-resolution MS/MS (LC–HRMS) was performed with an IQ-X Tribrid Orbitrap mass spectrometer (ThermoFisher Scientific, Waltham, MA, USA) equipped with a Thermo Scientific™ OptaMax™ NG heated electrospray ionization interface (ThermoFisher Scientific, Waltham, MA, USA) connected to an Vanquish Duo LC system including a binary pump, autosampler, and column oven (ThermoFisher Scientific, Waltham, MA, USA).

Analyses were performed with an Acquity UPLC CSH C18 column (50 × 2.1 mm, 1.7 μm; Waters, Milford, MA, USA) with column temperature set to 30 °C with mobile phases A H_2O + 0.1 % v/v formic acid and 10 mM ammonium formate and B 95:5 CH3CN:H2O + 0.1 % v/v formic acid and 10 mM ammonium formate. A flow rate of 0.3 mL min^{-1} was set, with initial conditions of 30 % B held for 0.5 min. A linear gradient elution to 50 % B over 7.5 min was set, then held for 2.5 min before being increased to 70 % B over 10.0 min. This was then increased to 99 % B over 0.5 min and held at 99 % B for 1.5 min, then returned to initial conditions over 0.5 min and held for 2.0 min to equilibrate the system prior to the next injection. The flow was diverted to waste after 24 min. Total run time was 25 min, with an injection volume of 5.0 μL. The column was connected to a pre column heater (Thermo Fisher Scientific, Waltham, MA, USA) equilibrated under flow to 30 °C and kept in a column oven set to 30 °C.

In positive ion mode, the mass spectrometer was calibrated from *m/z* 42–1822, the spray voltage was set to 3.5 kV, the capillary temperature and vaporizer temperature was set to 300 °C and 350 °C, and the sheath, auxiliary and cone gas flow rates were 43, 10 and 1 units, respectively, with MS data acquired from 0.5 to 24 min. Mass spectral data was collected using a combined FS/DDA method. FS data was collected from *m/z* 67–1000 using the 120,000 resolution setting, an isolation window of 1.6 *m/z* using the quadrupole isolation mode, an AGC target of 250 % (1×10^6), and a max injection time of 100 ms. Collision induced dissociation (CID) spectra were recorded using a DDA unscheduled target list which included *m/z* values 830.5049, 816.4893, 846.4998, 802.4736, 860.4791, 832.4842, 876.4741, 846.4634 and 818.4685 with a tolerance of 5.0 ppm. Data was collected using the 30,000 resolution setting, an AGC target of 200 % (1×10^5), max injection time set to 54 and HCD of 45 %.

2.10. Heating study

A heating study was performed to investigate the potential decarboxylation of some AZA derivatives produced during cooking. Six portions (50 μL each) of the same replicate of hepatopancreas extract were transferred to HPLC vials containing a 200 μL glass insert (Agilent, Santa Clara, CA, USA). 3 replicates were placed in the auto sampler and held 4.0 °C. The remaining 3 were heated at 90 °C for 10 min before being placed in a Vanquish Duo auto sampler (Thermo Fisher Scientific, Waltham, MA, USA). Analysis of full scan total ion chromatogram peak areas was used to determine the decrease in abundance of carboxylated metabolites.

2.11. Molecular network

A Thermo.raw file from the DDA targeted MS/MS analysis of the shellfish was converted to MzXML format using proteowizard's MSConvert, (32 bit, peak picking MS levels 1–2) and uploaded to GNPS and ran as a project under standard conditions with a minimum cosine score of 0.70 and at least 6 matched fragments to form an edge. The network was then visualized in Cytoscape for further editing and used to depict the *m/z* differences associated to each analogue.

3. Results and discussion

3.1. Microalgal culture

The cultured strain of *Am. languida* (Z-LF-9-C9) has already been described to produce AZA-38 and -39, AZA-39 being the major toxin characterized by $[M+H]^+$ *m/z* 816.48 (Wietkamp et al., 2019). The strain was cultured in a 180 L photo-bioreactor and allowed for the production of a culture with a concentration of 15–20 fg $cell^{-1}$ of AZA-39 and 10–15 fg $cell^{-1}$ of AZA-38 (ratio 1:0.8). At the time of this study the culture averaged 26,000 cells mL^{-1} (Salas et al., 2023).

3.2. Mussel feeding experiments

Biological replicates of mussels were submerged directly into four algal cultures (3 culture replicates and the control). They opened and began feeding within minutes. The mussels remained open for several hours, but some closed within an hour or two after initial submersion suggesting that feeding activity had ceased. Fig. 2 shows the decreasing density of *Am. languida* cells once exposed to the mussels over a 24 h period.

The highest clearance rate of microalgal cells in the presence of mussels was recorded during the first hour with cell density being reduced by 20.2 % in average (5300 cells mL^{-1} h^{-1}). Afterwards, the clearance rate declined exponentially (15.1 % - 2 h, 7.9 % - 3 h, 14.6 % - 4 h, 7.5 % - 5 h), considering the concentration of cells at each time point as a percentage of the initial concentration. In a previous feeding study performed with *Az. spinosum*, Salas et al. noted that, at similar initial algal cell densities (30,000 cells mL^{-1}), culture volume (5 L) and less mussels per replicate (n = 3), a reduction of algae to 5000 cells mL^{-1} after 3 h was observed, a much higher clearance rate compared to our study (Fig. 2). (Tillmann et al., 2017; Salas et al., 2011) The lower clearance rate observed in our experiment may have been a physiological response from the mussels to the presence of the toxigenic species or

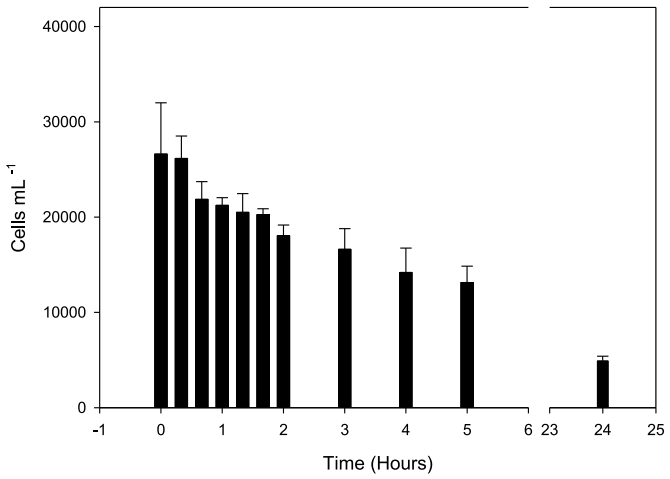

Fig. 2. Cell densities of *Am. languida* over 24 h during a feeding study with blue mussels.

some components of the culture media. The filtration rate was calculated to be 38.1 mL h^{-1} per mussel over the 24 h experiment and was significantly lower than the previously published range of 94–116 mL h^{-1} per mussel during a feeding study with *Az. poporum* (Krock et al., 2024). Past feeding studies by Jauffrais et al. have suggested that higher density monoculture feeding studies may reduce the feeding rate of shellfish and indicated that wild feeding events may have the potential to accumulate higher levels of AZAs from lower concentration wild diets or biomagnification of AZAs from intermediary organisms, and over a longer period of time (Jauffrais et al., 2012).

3.3. Azaspiracid analysis of shellfish tissues

LC-MS/MS analyses of the control sea water and mussel tissues indicated an absence of AZA-38 and -39 before the first feeding of *Am. languida*. After 24 h, three mussels were harvested from each replicate container and from the control container with no algae. The mussels were dissected and their hepatopancreas and remaining tissues were analyzed by LC-MS/MS. The AZA content was quantified against AZA-1 to give a relative quantification of the toxins present. Fig. 3 shows the concentrations of AZA-38 and -39 determined in the mussel's hepatopancreas and remainder tissue. Larger amounts of AZA-38 and -39 were recovered from the hepatopancreas compared to the remainder tissue, indicating cell ingestion and highlighting that the hepatopancreas is the

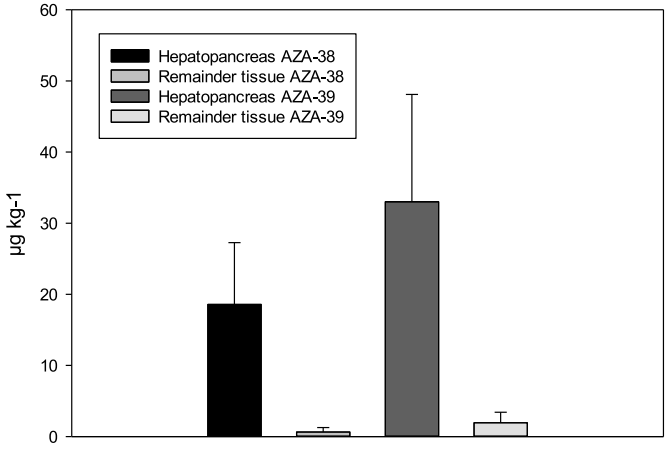

Fig. 3. AZA-38 and AZA-39 concentrations in µg kg^{-1} in the hepatopancreas and remainder tissues in the three replicates after 24 h with error bars showing standard deviation.

relevant tissue for use in quantitation studies. The combined concentrations of AZA-38 and AZA-39 were not found to exceed the regulatory limit as defined for the toxic AZA-1 (160 µg kg^{-1}). However, as no reference material is available for AZA-38 and -39, the relative response between both AZA-38 and -39 and AZA-1 is yet to be determined and might affect the quantification values.

The hepatopancreas tissue extracts prepared from the replicates containing the highest concentration of AZAs were then analyzed by LC-MS/MS for the detection of AZA derivatives produced by biotransformations in the shellfish tissue (Fig. 4). Common product-ions in the LC-MS/MS spectra of AZA-38 and AZA-39 belong to the groups 3, 4, 5 and 6 with *m/z* 448, 348, 248 and 154 respectively (Fig. 5). These product-ion groups differ from that the one of AZA-1 which are 14 Da (*m/z* 362, Fig. 4) larger due to the presence of an additional methyl on ring I (Fig. 1). (Krock et al., 2012) In a previous study, AZA-38 (*m/z* 830) was deemed to be a close analogue of AZA-37 (*m/z* 846) with similar fragments in their MS/MS spectra (Fig. 4). (Krock et al., 2015) The absence of the hydroxyl group at C-3 of the side-chain for AZA-38 was the only structural difference between the analogues, which was further evidenced by the prominent loss of CO_2 (43.9898 Da) for AZA-37. The methyl group, originally postulated to be at C-3, was instead placed at C-14 to conform to the observation that no neutral loss of CO_2 was present in the MS/MS spectra of AZA-38. The structure of AZA-37 was later confirmed by NMR and shares the same *m/z* 348 product-ion. No other AZAs elucidated with NMR have exhibited a loss of the C-14 methyl, which makes it unlikely that AZA-38 is without a methyl at this location. No typical group 2 fragments are observed for both AZA-37 and -38 at *m/z* 672. Instead, a product ion at *m/z* 686 $[M–144+H]^+$ was present that could not correspond to the postulated retro-Diels–Alder cleavage of AZA-1 in the presence of a fully saturated ring A in AZA-37 and -38 (Fig. 5). (Krock et al., 2015)

The molecular formula of AZA-39 is consistent with a loss of a methylene when compared to AZA-38. However, the fragmentation pattern of these two compounds differs with the absence of the $[M + H–144]^+$ product ion (*m/z* 686) in the CID spectrum of AZA-39 and the presence of a decarboxylation with a fragment at $[M + H–44]^+$. Initial loss of CO_2 was also observed in AZA-37 (Krock et al., 2015). Interestingly, AZA-39 loses CO_2 in a much higher ratio than AZA-37 with $[M + H–44–H_2O]^+$ being the largest product-ion in the CID spectrum for AZA-39 compared to AZA-37 where that largest fragment ion is $[M + H–H_2O]^+$. This suggests that the proximity of the olefinic carbons to the carboxylic acid might stabilize the loss of CO_2. The structure of AZA-39 has recently been elucidated using NMR and exhibits a 5-membered ring A (Fig. 5) instead of the 6-membered ring, typical of AZAs (Salas et al., 2023). Shellfish metabolites of AZA-38 and -39 (Fig. 5) were also detected in the mussel tissue extracts and their structures were proposed based on their MS/MS product-ion spectra. These shellfish metabolites shared some or most of the product-ions observed with AZA-38 and -39 (Fig. 6). We observed similar shellfish metabolism of AZA-38 and -39 than what was previously reported for AZA-1 and -2 in blue mussels (Salas et al., 2011), We determined oxidation, decarboxylation and hydroxylation as transformation routes for both AZA-38 and AZA-39 leading to eight new postulated AZA derivatives named AZA-80 to −87.

Retention times (rt) of the shellfish metabolites were shifted from those seen for AZA-38 and -39 (Fig. 6). As the polar surface area is increased by the shellfish metabolism, earlier elution was observed for most metabolites. Fig. 6b shows the proposed pathway for the formation of the biotransformed products of AZA-38 and -39 in the shellfish, similar to what Jauffrais et al. observed for AZA-1 and -2 (Jauffrais et al., 2012).

The hydroxylated analogues of both AZA-38 and AZA-39 named AZA-80 ($[M+H]^+$ *m/z* 846.4987, $C_{46}H_{72}NO_{13}^+$, Δ −1.3 ppm) and AZA-84 ($[M+H]^+$ *m/z* 832.4840, $C_{45}H_{70}NO_{13}^+$, Δ −0.2 ppm) were observed in the mussel tissue, with 15.9938 Da and 15.9950 more than AZA-38 and -39 respectively (Fig. 7). Similarly to the reported metabolism of AZA-1 (Kilcoyne et al., 2018), we propose that hydroxylation occurs on ring E,

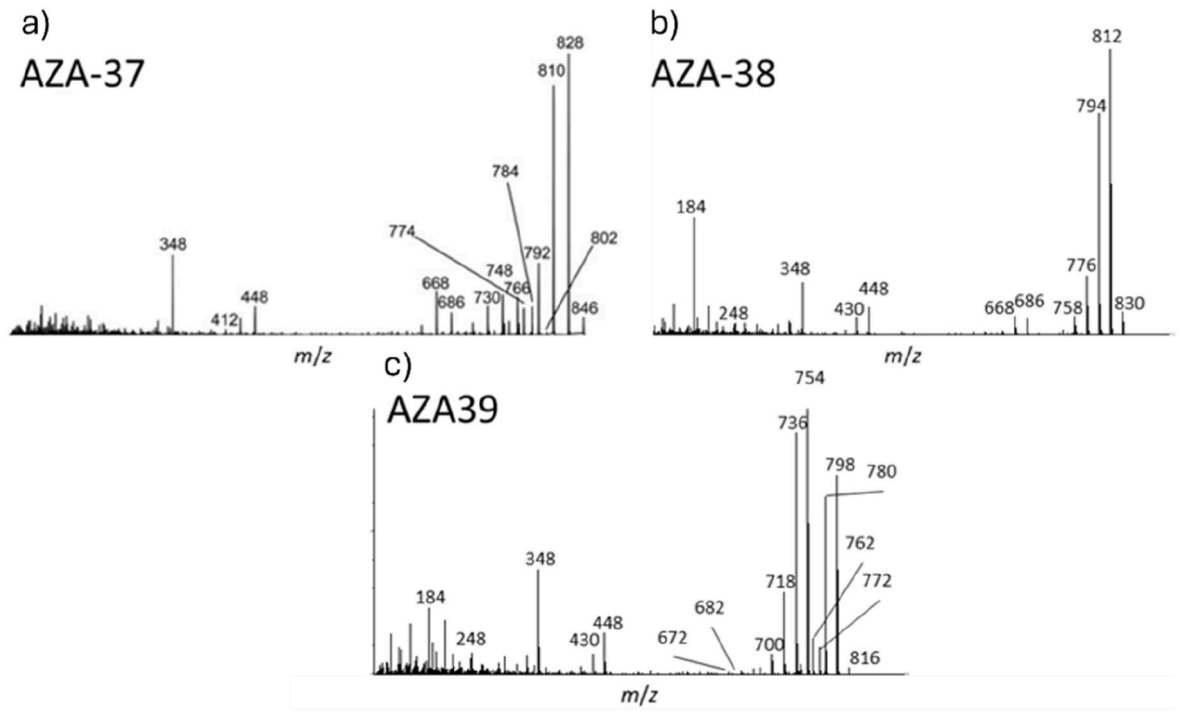

Fig. 4. a) CID spectrum of AZA-37 by Krock et al. and b–c) CID spectra recorded during this study (Krock et al., 2015).

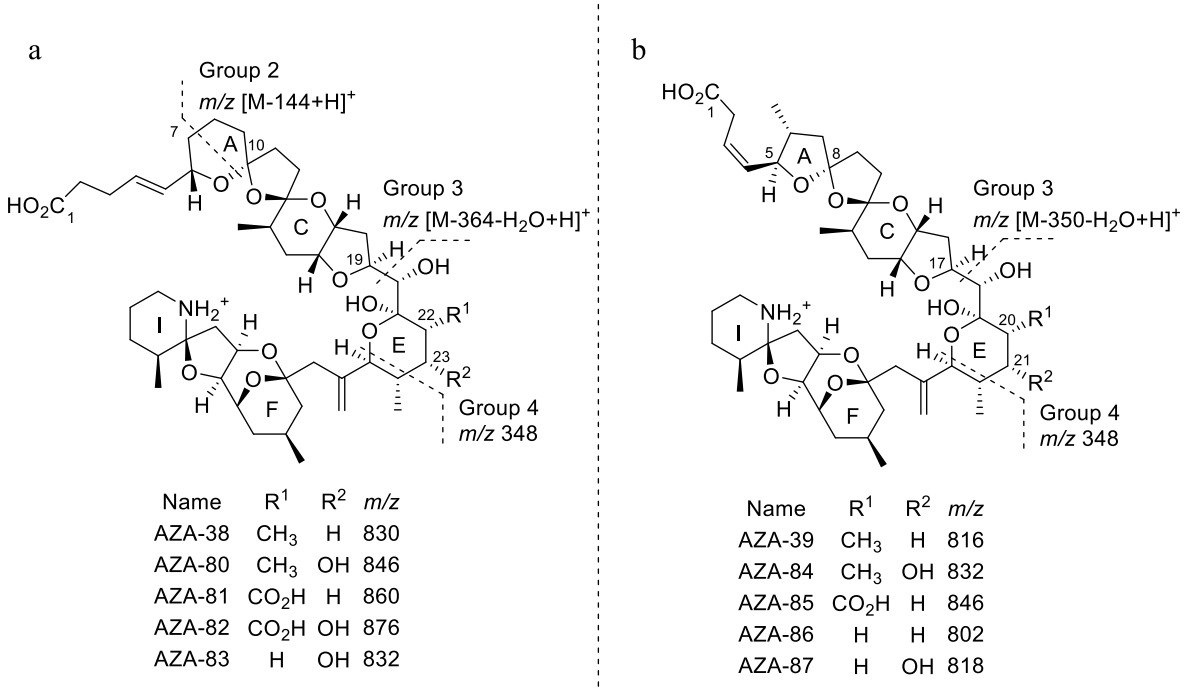

Name	R^1	R^2	*m/z*
AZA-38	CH_3	H	830
AZA-80	CH_3	OH	846
AZA-81	CO_2H	H	860
AZA-82	CO_2H	OH	876
AZA-83	H	OH	832

Name	R^1	R^2	*m/z*
AZA-39	CH_3	H	816
AZA-84	CH_3	OH	832
AZA-85	CO_2H	H	846
AZA-86	H	H	802
AZA-87	H	OH	818

Fig. 5. Fragmentation pattern for a) AZA-38 and b) AZA-39 and the putative structures of the new derivatives AZA-80 to −87. Assumed stereochemistry of AZA-38 to follow AZA-3 from C-13 to C-40. NB AZA38 and AZA39, and their respective metabolites, have different atom numbering due the difference in the number of carbon atoms they contain.

at C-23 for AZA-38 and C-21 for AZA-39. Both compounds, AZA-80 and AZA-84, showed the same pattern of fragmentation for group 3, which exhibited an additional water loss indicated by fragments at *m/z* 464.2987 ($C_{26}H_{42}NO_6^+$, Δ −4.2 ppm) and 464.2993 ($C_{26}H_{42}NO_6^+$, Δ −2.9 ppm) respectively (Table 1), and is consistent with the presence of a hydroxyl group at this position. Similar fragmentation patterns were observed for the hydroxylated products of AZA-1 and AZA-2 named AZA-5, AZA-8 and AZA-10 (Kilcoyne et al., 2015a).

AZA-81 and -85 were present as the carboxylated analogues of AZA-38 and -39 respectively. AZA-81 ($[M+H]^+$ *m/z* 860.4792, $C_{46}H_{70}NO_{14}^+$, Δ −0.3 ppm) had a fragmentation pattern characteristic of a decarboxylation with a neutral loss of 43.9898 Da in the product-ion spectrum. The MS/MS data suggest that this compound corresponds to the carboxylated product at C-22 of AZA-38 (Fig. 7). The loss of CO_2 is not

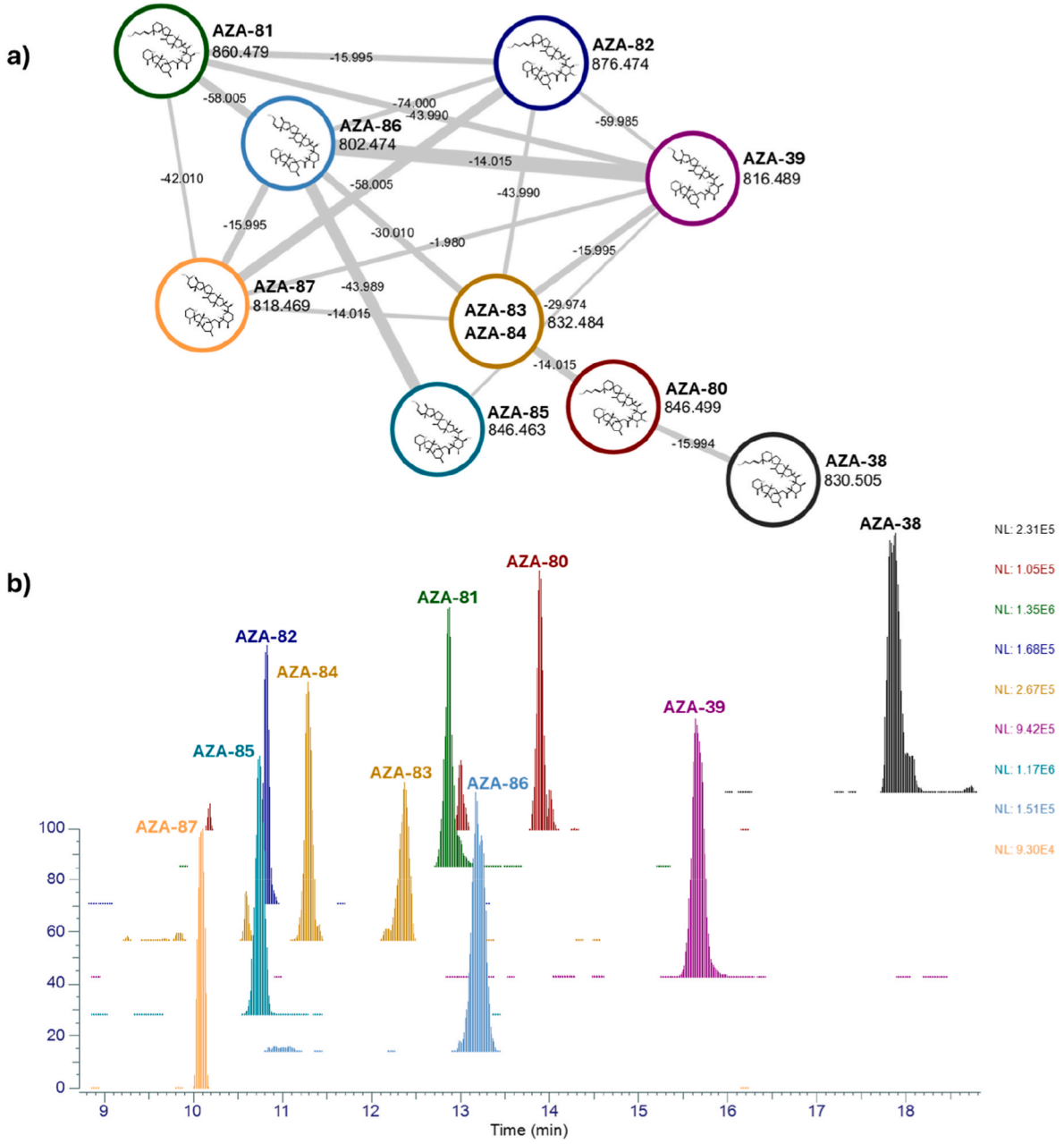

Fig. 6. a) Molecular network for visualization of mass differences between AZA-38—88 and b) Normalised extracted-ion full-scan chromatographic separation of AZA-38 (17.9 min), AZA-39 (15.6 min), AZA-80 (13.9 min), AZA-81 (12.9 min), AZA-82 (10.8 min), AZA-83 (12.4 min), AZA-84 (11.3 min), AZA-85 (10.7 min), AZA-86 and (13.2 min), AZA-87 (10.1 min).

common for the AZA-38 metabolites and could be explained by the presence of a second carboxylic acid group. As expected, the usual group 3 fragment was not present at *m/z* 448 but it was replaced by a product-ion at *m/z* 434.2902 ($C_{25}H_{40}NO_5$+, Δ −0.2 ppm) indicative of the oxidation of the C-22 methyl followed by a loss of CO_2 (Table 1). AZA-85 ($[M+H]^+$, *m/z* 846.5021, $C_{45}H_{68}NO_{14}^+$, Δ −0.5 ppm) showed a decarboxylation indicated by the neutral loss of 43.9898 Da and product-ion at *m/z* 784.4615 ($[M + H–H_2O–CO_2]^+$, $C_{44}H_{66}NO_{11}^+$, Δ −2.0 ppm). A second neutral loss of 43.9898 was also observed in the CID spectrum (Fig. 7) and was the most abundant at *m/z* 740.4721 ($[M + H–2CO_2–H_2O]^+$, $C_{43}H_{66}NO_9^+$, Δ −1.5 ppm). Similar to AZA-81, the group 3 fragment was present with *m/z* 434.2900 ($C_{25}H_{40}NO_9^+$, Δ −0.2 ppm) indicating the absence of the methyl group at C-20 and likely position of the carboxylation at C-20.

AZA-82 ($[M+H]^+$, *m/z* 876.4733, $C_{46}H_{70}NO_{15}^+$, Δ −0.8 ppm) was observed in the mussel tissue extracts, corresponding to the 23-hydroxylated metabolite of the 22-carboxylated AZA-81. The most abundant product-ion at *m/z* 796.4620 ($[M + H–CO_2–2H_2O]^+$, $C_{45}H_{66}NO_{11}^+$, Δ −1.3 ppm) is reminiscent of the CID fragment pattern of AZA-81 which exhibits the most abundant fragment ion at *m/z* 798.4775 ($[M + H–CO_2–H_2O]^+$, $C_{45}H_{68}NO_{11}^+$, Δ −1.5 ppm). The group 3 fragment indicated that the additional hydroxyl group is easily lost during CID leaving just the carboxylated product-ion at *m/z* 476.2636 ($C_{26}H_{38}NO_7^+$, Δ −1.4 ppm) followed by the neutral loss of 43.9898 Da ($[M+H]^+$, *m/z* 432.2736, $C_{25}H_{38}NO_6^+$, Δ −2.0 ppm) consistent with the loss of CO_2 (Table 1). The *m/z* ratio of 432.2736 indicates that loss of two protons and presence of two additional olefinic carbons when compared to AZA-81. Fragment group 4 at *m/z* 348.2526 was intact and with the unusual presence of the olefinic carbons helped isolate the change in structure to ring I where hydroxylation to C-22 have already been observed for AZA-

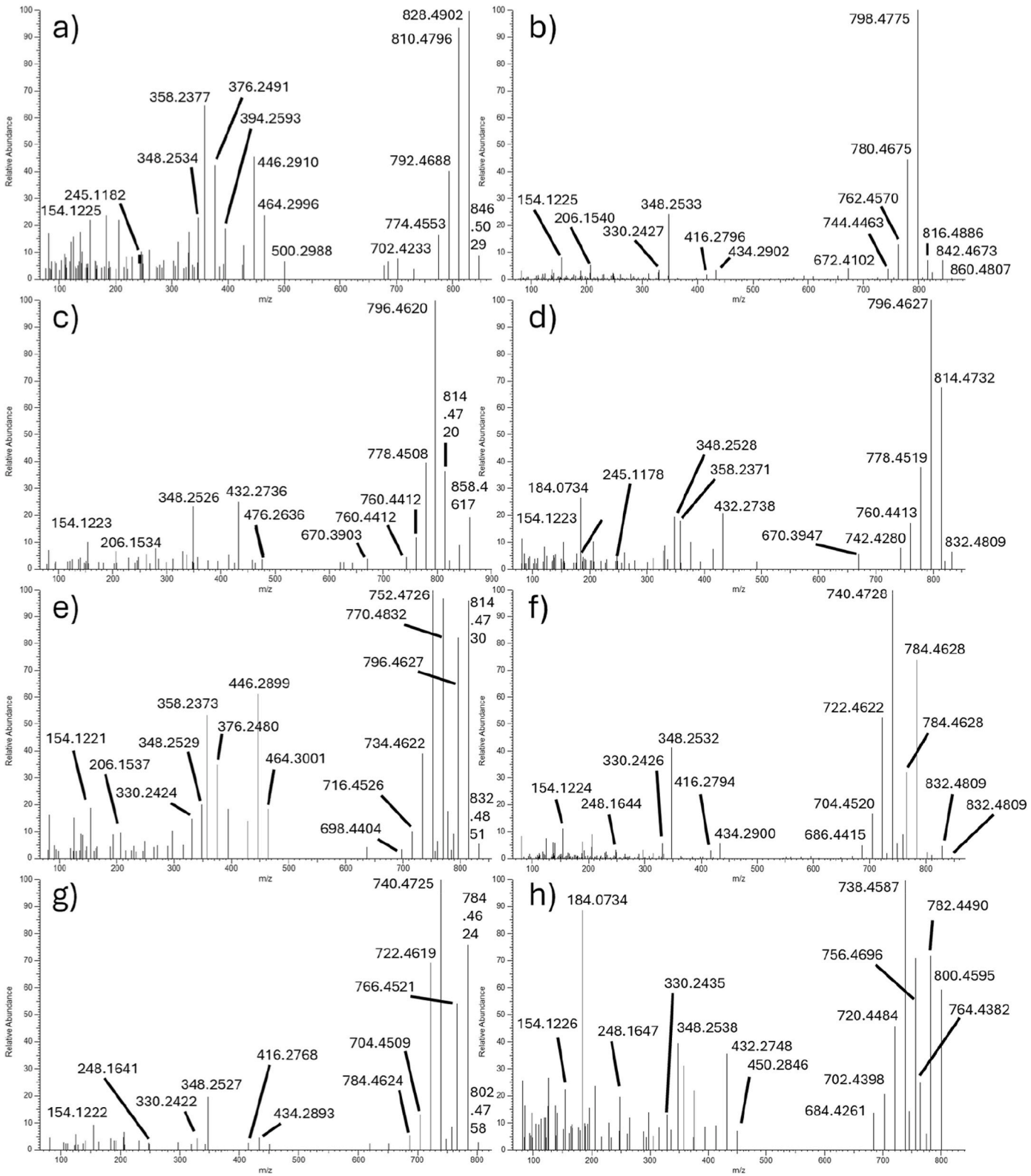

Fig. 7. CID spectra of detected azaspiracids, indicating major fragments. (a) AZA-80, (b) AZA-81, (c) AZA-82, (d) AZA-83, AZA-84, (b) AZA-85, (c) AZA-86, (d) AZA-87.

1 (Kilcoyne et al., 2015a).

Two compounds AZA-83 ($[M+H]^+$ *m/z* 832.4840, $C_{45}H_{70}NO_{13}^+$, Δ −0.3 ppm) and AZA-87 ($[M+H]^+$ *m/z* 818.4683, $C_{44}H_{68}NO_{13}^+$, Δ −0.3 ppm) were postulated to be the decarboxylated (neutral loss of 43.9898 Da) analogues of AZA-82 and AZA-85, respectively. Both compounds were 1.9833 Da more than AZA-38 and -39, corresponding to a loss of the C-22 methyl and an additional hydroxy group present. The location of the hydroxylation on AZA-83 and -87 was identified by the presence of the group 4 fragment at *m/z* 432.2738 ($C_{25}H_{38}NO_5^+$, Δ −1.5 ppm) and *m/z* 432.2762 ($C_{25}H_{38}NO_5^+$, Δ 0.8 ppm) indicating the presence of two

Table 1
Accurate mass measurements of $[M+H]^+$ and fragment 3.

Compound	RT	$[M+H]^+$			Fragment Group 3		
		m/z	Composition	ppm	*m/z*	Composition	ppm
AZA-38	4.36	830.5051	$C_{46}H_{72}NO_{12}^+$	0.2	448.3064	$C_{26}H_{42}NO_5^+$	1.4
AZA-80	3.57	846.5003	$C_{46}H_{72}NO_{13}^+$	0.6	464.2987	$C_{26}H_{42}NO_6^+$	-4.2
AZA-81	3.49	860.4792	$C_{46}H_{70}NO_{14}^+$	0.1	434.2893	$C_{25}H_{40}NO_5^+$	-1.8
AZA-82	3.16	876.5021	$C_{46}H_{70}NO_{15}^+$	-20.9	432.2744	$C_{25}H_{38}NO_5^+$	-0.1
AZA-83	3.38	832.4836	$C_{45}H_{70}NO_{13}^+$	-0.7	432.2724	$C_{25}H_{38}NO_5^+$	-4.7
AZA-39	3.99	816.4883	$C_{45}H_{70}NO_{12}^+$	-1.2	448.3061	$C_{26}H_{42}NO_5^+$	0.8
AZA-84	3.14	832.4840	$C_{45}H_{70}NO_{13}^+$	-0.2	464.2993	$C_{26}H_{40}NO_5^+$	-2.9
AZA-85	3.19	846.4601	$C_{45}H_{68}NO_{14}^+$	-3.9	434.2905	$C_{25}H_{40}NO_5^+$	0.9
AZA-86	3.56	802.4741	$C_{44}H_{68}NO_{12}^+$	0.6	434.2877	$C_{25}H_{40}NO_5^+$	-5.5
AZA-87	3.97	818.4691	$C_{44}H_{68}NO_{13}^+$	0.7	432.2721	$C_{25}H_{38}NO_5^+$	-5.4

Table 2
Azaspiracid toxin budget.

Replicates	Culture at T0 (ng)	Final AZA Concentration in Filtrate at T24 (ng)	Tissue after 24 h (ng)[a]						Bio-deposits (ng)					Total (ng)	%
	AZA-38	AZA-38	AZA-81	AZA-38	AZA-80	AZA-81	AZA-82	AZA-83	AZA-38	AZA-80	AZA-81	AZA-82	AZA-83	Recovered	
24405 R1	3596.5	1382.2	8.5	82.5	13.2	563.4	<LOQ	12.9	109.0	<LOQ	4.8	<LOQ	<LOQ	2176.5	60.5
24830 R2	3675.7	1316.8	52.8	57	18	823.8	<LOQ	28.5	64.0	<LOQ	0.7	<LOQ	<LOQ	2361.6	64.2
30616 R3	3227.1	1293.2	95.4	106.8	26.4	303.3	<LOQ	18.3	121.4	<LOQ	17.1	<LOQ	<LOQ	1981.9	61.4
Mean	3499.8	1330.7	52.2	82.1	19.2	563.5	<LOQ	19.9	98.1	<LOQ	7.5	<LOQ	<LOQ	2173.1	62.0
% toxins in mussel tissue															19.6
% toxins in suspended particulate matter															39.5
% toxins in bio-deposits															3.0

Replicates	Culture at T0 (ng)	Final AZA Concentration in Filtrate (ng)		Tissue after 24 h (ng)[a]						Bio-deposits (ng)					Total (ng)	%
Replicates	AZA-39	AZA-39	AZA-84	AZA-87	AZA-39	AZA-84	AZA-85	AZA-86	AZA-87	AZA-39	AZA-84	AZA-85	AZA-86	AZA-87	Recovered	
24405 R1	6636.3	3673.2	643.0	850.8	169.2	46.2	431.7	25.2	33.0	113.4	<LOQ	LOQ	15.4	9.2	6010.3	90.6
24830 R2	6336.2	4668.3	483.0	796.8	113.1	69.0	712.2	33.9	11.4	87.2	<LOQ	40.0	23.0	<LOQ	7037.9	111.1
30616 R3	5095.9	3024.8	<LOQ	<LOQ	183.3	107.4	480.6	18.6	20.7	84.6	<LOQ	42.7	35.8	<LOQ	3998.5	78.5
Mean	6022.8	3788.8	375.4	549.2	155.2	74.2	541.5	25.9	21.7	95.1	<LOQ	27.6	24.7	3.07	5682.2	94.3
% toxins in mussel tissue																13.6
% toxins in suspended particulate matter																78.3
% toxins in biodeposits																2.5

LOD is 0.003 μg g^{-1} and LOQ is 0.005 μg g^{-1}.
[a] Values were multiplied by 3 to represent the 9 mussels contained in each replicate.

olefinic carbons that resulted from a loss of H_2O. Interestingly, we did observe a hydroxylated group 4 product-ion at *m/z* 450.2846 ($C_{25}H_{40}NO_6^+$, Δ −0.9 ppm) in the CID spectrum for AZA-87 but not for AZA-83.

Finally, AZA-86 ($[M+H]^+$ *m/z* 802.4736, $C_{44}H_{68}NO_{12}^+$, Δ −0.0 ppm) was postulated to be the demethylated derivative of AZA-39 as it exhibited a single initial loss of CO_2, with a fragment ion at *m/z* 740.4725 ($[M + H–CO_2–H_2O]^+$, $C_{43}H_{66}NO_9^+$, Δ −1.0 ppm), common for non-carboxylated AZA-39 metabolites (Fig. 7). Comparing to AZA-39 all typical fragmentation groups were conserved with the exception of group 3 which lacked one methylene unit with *m/z* 434.2893 ($C_{25}H_{40}NO_5^+$, Δ −1.8 ppm) compared to *m/z* 448.3062 in AZA-39 and suggested that AZA-86 is the demethylated product of AZA-39 at position C-22. This metabolite is likely formed through a decarboxylative process to the oxidized product of AZA-39 at the methyl located at C-22 as already proposed for the oxidative products of AZA-1 and -2.

LC-MS/MS quantification of the AZA metabolites was performed on the culture at the start of the experiment (T0), particulate-free supernatant (T24), on the tissue extracts and the bio-deposits (Table 2). Most of the toxin was recovered in the particulate-free supernatant as AZA-38 and -39 along with the 22-carboxylated analogues which were the major metabolites present (Table 2, refer to Fig. 5 for structures). Higher ratios of 22-carboxylated analogues were found in the particulate-free supernatant than in the tissue extracts. Recovery of the initial toxin quantities varied greatly between replicates and as did the yield of AZA-38 and -39. AZA-39 had much higher recovery yields when compared to AZA-38. Concentrations of metabolites found in the pseudo-faeces and filtered particulate matter were very low with many being below the limits of accurate quantitation.

As seen in the previous feeding study using AZA-1 and *Az. spinosum* (Salas et al., 2011), both AZA-81 and -85 were the most abundant shellfish metabolites with ratios of 1:6.9 (AZA-38:AZA-81) and 1:3.5 (AZA-39:AZA-85) in shellfish tissue. The majority of AZA-81 and -85 were present in the remainder tissue with ratios of 1:2.1 (AZA-38: AZA-80) and 1:2.8 (AZA-39:AZA-85) (Table 3). This compares to reported ratios of AZA-1:AZA-17, which found higher levels of AZA-17 in the remainder tissue than in the hepatopancreas (Salas et al., 2011). Total concentrations of the AZA metabolites in the shellfish tissue remained below regulatory limits (160 μg kg^{-1}) again in contrast to previous feeding studies (Salas et al., 2011).

Heating studies were used to confirm the presence of the carboxylic acid group and to simulate the effects of cooking. Cooking can lead to total or partial decarboxylation of the carboxylated shellfish metabolites and can be used to confirm their presence. Previous studies have shown

Table 3
AZA content present in whole mussel tissue per replicate after 24 h.

	AZA-38	AZA-39	AZA-80	AZA-81	AZA-82	AZA-83	AZA-84	AZA-85	AZA-86	AZA-87	Total
	μg kg^{-1}	μg kg^{-1}	μg kg^{-1}	μg kg^{-1}	μg kg^{-1}	μg kg^{-1}	μg kg^{-1}	μg kg^{-1}	μg kg^{-1}	μg kg^{-1}	μg kg^{-1}
R1	16.84	31.00	0.27	10.85	0.07	0.25	0.97	9.15	0.58	0.67	70.65
R2	16.28	30.60	0.31	15.28	0.01	0.42	1.28	13.98	0.51	1.04	79.71
R3	32.70	57.55	0.46	11.57	0.02	0.32	2.04	10.37	0.22	LOQ	115.24
Average	21.94	39.72	0.35	12.57	0.03	0.33	1.43	11.17	0.44	0.86	88.53

that decarboxylation of carboxylated azaspiracid analogues occurs readily when heated (Kilcoyne et al., 2015a). Carboxylated AZA-17, -21, −19 and −23 were shown to convert to their decarboxylated products AZA-3, -4, -6 and -9 in previous heating studies (Kilcoyne et al., 2015a). These decarboxylated analogues can be more toxic and of concern as the 22-demethylated AZA-6 was several times more toxic than AZA-19 using a Jurkat T-lymphocyte assay (Kilcoyne et al., 2015b). A replicated trial was performed to further confirm the presence of the carboxylic acid group on AZA-81, -82 and −84. The shellfish sample was divided into two separate groups, with one group being heated. A reduction in the abundance of AZA-81, 82 and −85 was observed in the heated sample compared to the sample that was not heated (Fig. 8).

Finally, analysis of shellfish tissue extracts was performed to identify whether AZA-38 and -39 were present in samples that were provided for routine analysis to the national monitoring program in Ireland. Table 4 shows quantitative data indicating the locations where AZA-38 and -39 were present in shellfish tissues during the period from the 26th of October until November 2, 2020. Several locations on Ireland's south-west coast highlighted below tested positive for levels of AZA-38 and -39 and therefore suggests that concentrations of *Am. languida* cells might have been present (Table 4). A review of the harmful algal bloom bulletin produced by The Marine Institute of Ireland (2020, week 46) indicated there were *Azadinium* like species present in waters off the southwest coast of Ireland in the weeks leading up to the routine sampling of farmed shellfish used in our analysis (Harmful Algae Bloom Bulletin, 2020). Two species commonly farmed, *M. edulis* and *Pecten maximus* were found to have accumulated the AZAs. Concentrations were below the regulatory limits for AZA-1 equivalents and a magnitude lower in concentration than AZA-1 also present in the tissue. Although no shellfish intoxication incidents relating to the AZA-38 and -39 producing strain of *Am. languida* have been reported thus far, shellfish intoxications reaching >500 μg AZA-1 eq. kg^{-1} caused by the Andalusian strain of *Am. languida,* producing AZA-2 and -43, has occurred (Tillmann et al., 2017). A 2017 survey of Irish waters found combined concentrations of AZA-38 and -39 reaching 4.9 and 2.8 ng L^{-1} respectively in the seawater along transects protruding from Bantry Bay and east along the Crease Line transect (McGirr et al., 2022). During the same survey, concentrations of the regulated AZA-1, -2 and -33 reached a maximum of 1.1 ng L^{-1} in seawater and importantly highlighted that AZA-38 and -39 should be considered for routine monitoring. Our analysis also showed that shellfish originating from Bantry Bay contained AZAs and indicates it might be a region of interest for further monitoring. This is the first reported case of AZAs not originating from *Az. spinosum* intoxicating Irish shellfish that are not yet routinely monitored for. As concentrations were always low, it would be inappropriate to overstate the risk associated with these findings. However, it highlights the need for further studies on the toxins produced by *Am. languida* associated to Irish waters to determine the toxicity of both AZA-38 and -39.

Table 4
Shellfish harvesting sites that tested positive for AZA-38 and -39.

			Concentration AZA-1 equiv. (μg g^{-1})		
Shellfish species	Sampling site	Sampling Date	AZA-1	AZA-38	AZA-39
M. edulis	Bantry Middle	26/10/2020	0.065	0.002	0.005
M. edulis	Bantry South	26/10/2020	0.070	0.002	0.004
M. edulis	Dunmanus Bay	26/10/2020	0.012	0.000	0.001
M. edulis	Bantry North	26/10/2020	0.040	0.002	0.006
M. edulis	Glengarriff	27/10/2020	0.022	0.002	0.007
M. edulis	Castletownbere	26/10/2020	0.010	0.002	0.009
M. edulis	Newtown	26/10/2020	0.060	0.000	0.005
M. edulis	Adrigole	27/10/2020	<LOQ	0.000	0.007
Pecten maximus	Castletownbere	26/10/2020	<LOD	0.004	0.007
M. edulis	Castletownbere	01/11/2020	0.015	0.001	0.008
M. edulis	Castletownbere	01/11/2020	0.012	0.002	0.011
M. edulis	Glengarriff	01/11/2020	0.033	0.002	0.007
M. edulis	Bantry North	02/11/2020	0.034	0.003	0.007
M. edulis	Bantry Middle	02/11/2020	0.041	0.001	0.004
M. edulis	Bantry South	02/11/2020	0.059	0.002	0.004

LOD is 0.003 μg g^{-1} and LOQ is 0.005 μg g^{-1}.

4. Conclusions

So far, azaspiracids AZA-1 and -2 contamination events in Ireland have been an issue associated with the presence of the dinoflagellate *Az.*

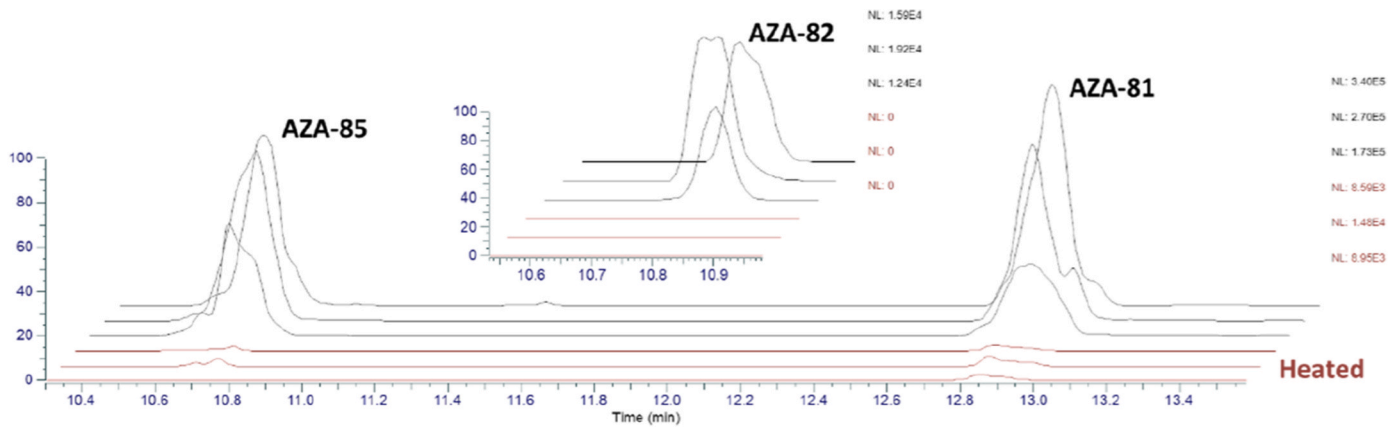

Fig. 8. Extracted total ion chromatograms of AZA -81, −82 and −85 in heated and non-heated extracts.

spinosum. *Am. languida* has so far been observed in Irish and Norwegian coastal waters as well as the North Atlantic, where a bloom has already been recorded in a recent survey (Wietkamp et al., 2020). As the Spanish population of *Am. languida* has already been associated with a shellfish intoxication event, and with farmed shellfish already showing trace amounts of AZA-38 and -39 in Ireland, more work should be undertaken to determine the potential toxicity of AZA-38, -39 and their biotransformed products. Although we are confident of the proposed structures of the shellfish metabolites using MS/MS fragmentation patterns, isolation and NMR analyses will be useful in order to confirm the structures of the eight new azaspiracids metabolites reported here. As a precaution, national monitoring programs in Ireland could include azaspiracid-38 and -39 treating their toxicity as that of AZA-1 until their toxicity is evaluated.

CRediT authorship contribution statement

Elliot Murphy: Writing – original draft, Methodology, Investigation, Formal analysis, Data curation. **Rafael Salas:** Writing – review & editing, Supervision, Resources, Methodology, Conceptualization. **Urban Tillmann:** Writing – review & editing, Resources. **Jane Kilcoyne:** Writing – review & editing, Validation, Software, Methodology, Data curation. **Bernd Krock:** Writing – review & editing, Data curation. **Olivier P. Thomas:** Writing – review & editing, Validation, Supervision, Resources, Project administration, Data curation.

Funding

EM has received financial support from a Cullen fellowship (Grant-Aid Agreement No. CF/18/03/01 of the Marine Institute and funded under the Marine Research Program by the Irish Government.

Declaration of competing interest

The authors declare the following financial interests/personal relationships which may be considered as potential competing interests: Olivier Thomas reports financial support was provided by Marine Institute. If there are other authors, they declare that they have no known competing financial interests or personal relationships that could have appeared to influence the work reported in this paper.

Acknowledgments

We would like to thank Christopher Miles for reviewing the manuscript and providing expert feedback on the structure elucidation.

Data availability

Data will be made available on request.

References

Alvarez, G., et al., 2010. First identification of azaspiracid and spirolides in *Mesodesma donacium* and *Mulinia edulis* from Northern Chile. Toxicon 55 (2–3), 638–641.
Álvarez-Muñoz, D., et al., 2016. Contaminants in the Marine environment. In: Blasco, J., et al. (Eds.), Marine Ecotoxicology. Academic Press, Amsterdam, pp. 1–34.
Brombacher, S., Edmonds S Fau - Volmer, D.A., Volmer, D.A., 2002. Studies on azaspiracid biotoxins. II. Mass spectral behavior and structural elucidation of azaspiracid analogs. Rapid Commun. Mass Spectrom. 16 (24), 2306–2316.
Economou, V., et al., 2007. Diarrheic shellfish poisoning due to toxic mussel consumption: the first recorded outbreak in Greece. Food Addit. Contam. 24 (3), 297–305.
Frost, B.W., 1972. Effects of size and concentration of food particles on the feeding behavior of the marine planktonic copepod *Calanus pacificus*. *Limnology and oceanography*, 17 (6), 805–815.
Furey, A., et al., 2010. Azaspiracid poisoning (AZP) toxins in shellfish: toxicological and health considerations. Toxicon 56 (2), 173–190.
Gerssen, A., et al., 2010. Marine toxins: chemistry, toxicity, occurrence and detection, with special reference to the Dutch situation. Toxins (Basel) 2 (4), 878–904.
Harmful Algae Bloom Bulletin, 2020. week 46 04/01/2025. Available from: https://www.marine.ie/site-area/data-services/interactive-maps/weekly-hab-bulletin#pdfviewer.
Hoagland, P., Scatasta, S., 2006. The economic effects of harmful algal blooms. In: Granéli, E., Turner, J.T. (Eds.), Ecology of Harmful Algae. Springer Berlin Heidelberg, Berlin, Heidelberg, pp. 391–402.
James, K.J., et al., 2003. Detection of five new hydroxyl analogues of azaspiracids in shellfish using multiple tandem mass spectrometry. Toxicon 41 (3), 277–283.
Jauffrais, T., et al., 2012. Azaspiracid accumulation, detoxification and biotransformation in blue mussels (*Mytilus edulis*) experimentally fed *Azadinium spinosum*. *Toxicon*, 60 (4), 582–595.
Kenton, N.T., et al., 2018. Stereochemical definition of the natural product (6R,10R,13R,14R,16R,17R,19S,20S,21R,24S,25S,28S,30S,32R,33R,34R,36S,37S,39R)-Azaspiracid-3 by total synthesis and comparative analyses. Angew. Chem. Int. Ed. 57 (3), 810–813.
Kilcoyne, J., et al., 2015a. Effects of heating on proportions of azaspiracids 1–10 in mussels (*Mytilus edulis*) and identification of carboxylated precursors for azaspiracids 5, 10, 13, and 15. J. Agric. Food Chem. 63 (51), 10980–10987.
Kilcoyne, J., et al., 2015b. Structure elucidation, relative LC-MS response and in vitro toxicity of azaspiracids 7-10 isolated from mussels (*Mytilus edulis*). J. Agric. Food Chem. 63 (20), 5083–5091.
Kilcoyne, J., et al., 2018. Identification of 21,22-Dehydroazaspiracids in mussels (*Mytilus edulis*) and in vitro toxicity of Azaspiracid-26. J. Nat. Prod. 81 (4), 885–893.
Kim, J.H., et al., Identification of Azadinium Species and a New Azaspiracid from *Azadinium Poporum* in Puget Sound, Washington State, USA. (1878-1470 (Electronic)).
Kittler, K., Preiss-Weigert, A., These, A., 2010. Identification strategy using combined mass spectrometric techniques for elucidation of phase I and phase II in vitro metabolites of lipophilic marine biotoxins. Anal. Chem. 82 (22), 9329–9335.
Krock, B., et al., 2008. LC-MS/MS aboard ship: Tandem mass spectrometry in the search for phycotoxins and novel toxigenic plankton from the north sea. Anal. Bioanal. Chem. 392 (5), 797–803.
Krock, B., et al., 2012. New azaspiracids in Amphidomataceae (Dinophyceae). Toxicon 60 (5), 830–839.
Krock, B., et al., 2015. Structure elucidation and in vitro toxicity of new azaspiracids isolated from the marine dinoflagellate *azadinium poporum*. *Marine drugs*, 13 (11), 6687–6702.
Krock, B., et al., 2019. Two novel azaspiracids from *Azadinium poporum*, and a comprehensive compilation of azaspiracids produced by Amphidomataceae, (Dinophyceae). Harmful Algae 82, 1–8.
Krock, B., et al., 2024. Azaspiracid-59 accumulation and transformation in mussels (*Mytilus edulis*) after feeding with *Azadinium poporum* (Dinophyceae). Toxicon 251, 108152.
Lehane, M., et al., 2004. Liquid chromatography–multiple tandem mass spectrometry for the determination of ten azaspiracids, including hydroxyl analogues in shellfish. J. Chromatogr. A 1024 (1–2), 63–70.
McCarron, P., et al., 2009. Formation of Azaspiracids-3, -4, -6, and -9 via decarboxylation of carboxyazaspiracid metabolites from shellfish. J. Agric. Food Chem. 57 (1), 160–169.
McGirr, S., et al., 2022. Co-localisation of azaspiracid analogs with the dinoflagellate species *Azadinium spinosum* and *Amphidoma languida* in the southwest of Ireland. Microb. Ecol. 83 (3), 635–646.
McMahon, T., Silke, J., 1996. Winter toxicity of unknown aetiology in mussels. Harmful Algae News 14, 2.
Nicolaou, K.C., et al., 2004. Structural revision and total synthesis of azaspiracid-1, part 2: definition of the ABCD domain and total synthesis. Angew. Chem. Int. Ed. 43 (33), 4318–4324.
Ofuji, K., et al., 1999. Two analogs of azaspiracid isolated from mussels, *Mytilus edulis*, involved in human intoxication in Ireland. Nat. Toxins 7 (3), 99–102.
Ofuji, K., et al., 2001. Structures of azaspiracid analogs, Azaspiracid-4 and Azaspiracid-5, causative toxins of azaspiracid poisoning in Europe. Biosci. Biotechnol. Biochem. 65 (3), 740–742.
O'Driscoll, D., et al., 2011. Mussels increase xenobiotic (Azaspiracid) toxicity using a unique bioconversion mechanism. Environ. Sci. Technol. 45 (7), 3102–3108.
Rehmann, N., Hess, P., Quilliam, M.A., 2008. Discovery of new analogs of the marine biotoxin azaspiracid in blue mussels (*Mytilus edulis*) by ultra-performance liquid chromatography/tandem mass spectrometry. Rapid Commun. Mass Spectrom. 22 (4), 549–558.
Rossi, R., et al., 2017. Mediterranean *Azadinium dexteroporum* (Dinophyceae) produces six novel azaspiracids and azaspiracid-35: a structural study by a multi-platform mass spectrometry approach. Anal. Bioanal. Chem. 409 (4), 1121–1134.
Salas, R., et al., 2011. The role of *Azadinium spinosum* (Dinophyceae) in the production of azaspiracid shellfish poisoning in mussels. Harmful Algae 10 (6), 774–783.
Salas, R., et al., 2023. Production of the dinoflagellate *Amphidoma languida* in a large scale photobioreactor and structure elucidation of its main metabolite AZA-39. Harmful Algae 127, 102471.
Sandvik, M., et al., 2021. In vitro metabolism of azaspiracids 1–3 with a hepatopancreatic fraction from blue mussels (*Mytilus edulis*). J. Agric. Food Chem. 69 (38), 11322–11335.
Satake, M., et al., 1998. Azaspiracid, a new marine toxin having unique spiro ring assemblies, isolated from Irish mussels. Mytilus edulis. Journal of the American Chemical Society 120 (38), 9967–9968.
Taleb, H., et al., 2006. First detection of azaspiracids in mussels in north west Africa. J. Shellfish Res. 25 (3), 1067–1070.

Tebben, J., et al., 2023. Structure and toxicity of AZA-59, an azaspiracid shellfish poisoning toxin produced by *Azadinium poporum* (Dinophyceae). Harmful Algae 124, 102388.
Tillmann, U., et al., 2009. *Azadinium spinosum* gen. et sp. nov. (Dinophyceae) identified as a primary producer of azaspiracid toxins. Eur. J. Phycol. 44 (1), 63–79.
Tillmann, U., et al., 2015. First record of *Azadinium dexteroporum* and *Amphidoma languida* (Amphidomataceae, Dinophyceae) from the Irminger Sea off Iceland. Marine Biodiversity Records 8, 11.
Tillmann, U., et al., 2017. *Amphidoma languida* (Amphidomatacea, Dinophyceae) with a novel azaspiracid toxin profile identified as the cause of molluscan contamination at the Atlantic coast of southern Spain. Harmful Algae 62, 113–126.
Tillmann, U., et al., 2018. Diversity, distribution, and azaspiracids of Amphidomataceae (Dinophyceae) along the Norwegian coast. Harmful Algae 80, 15–34.
Visciano, P., et al., 2016. Marine biotoxins: occurrence, toxicity, regulatory limits and reference methods. Front. Microbiol. 7, 1051.
Volmer, D.A., Brombacher, S., Whitehead, B., 2002. Studies on azaspiracid biotoxins. I. Ultrafast high-resolution liquid chromatography/mass spectrometry separations using monolithic columns. Rapid Commun. Mass Spectrom. 16 (24), 2298–2305.
Wietkamp, S., et al., 2019. Occurrence and distribution of amphidomataceae (Dinophyceae) in Danish coastal waters of the North sea, the Limfjord and the Kattegat/Belt area. Harmful Algae 88, 101637.
Wietkamp, S., et al., 2020. Distribution and abundance of azaspiracid-producing dinophyte species and their toxins in North Atlantic and North Sea waters in summer 2018. PLoS One 15 (6), e0235015.